scientific reports

Check for updates

OPEN

Rutin ameliorates sevoflurane-induced neurotoxicity by inhibiting microglial synaptic phagocytosis through the complement pathway

Xinyu Tian[1,6], Miaomiao Xiong[2,6], Zhiguo Jiang[3], Rong Hong[4] & Honghua Wang[1,5]✉

Repeated neonatal exposure to sevoflurane may impair synapses and lead to developmental neurobehavioral issues. In this study, we assessed the therapeutic effects of rutin on sevoflurane-induced neurotoxicity. The mice were exposed to 3% sevoflurane for 2 h daily on postnatal days (PNDs) 6, 8, and 10. The Morris water maze was used and an open field test was performed to assess the memory and anxiety-like behavior of the mice on PNDs 37–42. The effects of rutin on the complement cascade and microglial synaptic elimination in the hippocampus of mice were validated by Western blotting, real-time RT qPCR, morphological analysis, and immunohistochemistry examinations. The results showed that rutin effectively alleviated cognitive dysfunction and synaptic impairment in sevoflurane-treated mice. By decreasing microglial activation, rutin switched microglia from the ameboid phenotype to the ramified phenotype and decreased the phagocytic properties of microglia. Rutin treatment also rescued sevoflurane-induced synapse loss by preventing microglial synaptic engulfment through complements C1q and C3; this effect could be reversed by an extra C3 supplement. Our findings demonstrated that rutin could alleviate synapse loss and cognitive dysfunction in sevoflurane-treated mice by inhibiting complement-dependent microglial synapse phagocytosis. This provides a promising strategy for the prevention of sevoflurane-induced developmental neurotoxicity.

Keywords Sevoflurane, Neurotoxicity, Rutin, Microglial phagocytosis, C1q, C3

Anesthetic-induced developmental neurotoxicity is prevalent. During the early postnatal and childhood periods, a critical window of sensitivity to anesthetics, and exposure to general anesthesia may trigger neurotoxic changes in the developing brain[1,2]. Clinical studies have reported a link between early-life anesthesia exposure and neurocognitive dysfunction in adolescents, raising concerns about the safety of pediatric anesthesia[3–5]. Sevoflurane is an inhalational anesthetic widely administered to pediatric patients. Studies on rodents have shown that neonatal exposure to sevoflurane has deleterious effects on the brain[6–8]. Synaptic impairment is an important feature of sevoflurane-induced neurotoxicity. Sevoflurane decreases synaptic density, impairs synaptic transmission, and suppresses long-term potentiation induction[9–12].

Synapses are the fundamental structures of neural circuits that control brain functions and cognitive processes[13]. During postnatal development, microglia have a crucial role in synaptic formation, maturation, and elimination in the hippocampus, and deficient microglial synaptic engulfment results in an excess of dendritic spines and immature synapses[14–17]. Improper microglial activation and phagocytosis may result in neurocognitive disorders, such as Alzheimer's disease (AD), amyotrophic lateral sclerosis, and Huntington's disease[18–20]. Microglial phagocytosis depends on the complement system, which is a core mechanism for synaptic elimination in the developing brain[21] Activation of the complement system can result in proteolytic activation of the complement effector molecules C1q and C3, which bind to synapses and facilitate phagocytosis via the C3 receptor on microglia[22]. Recent studies reported that repeated or prolonged exposure to sevoflurane

[1]Institute of Anesthesiology, Suzhou Research Center of Medical School, Affiliated Hospital of Medical School, Suzhou Hospital, Nanjing University, Suzhou 215153, China. [2]Institute of Anesthesiology, Affiliated Hospital of Jiangnan University, Wuxi 214000, China. [3]Institute of Anesthesiology, The First People's Hospital of Yancheng, Affiliated Hospital of Medical School, Nanjing University, Yancheng 224000, Jiangsu, China. [4]Department of Radiology, Suzhou TCM Hospital Affiliated to Nanjing University of Chinese Medicine, Suzhou 215100, China. [5]Department of Anesthesiology, Affiliated Hospital of Medical School, Suzhou Hospital, Nanjing University, Suzhou 215100, China. [6]Xinyu Tian and Miaomiao Xiong have contributed equally to this work and share first authorship. ✉email: whhdc10@163.com

promoted microglial engulfment of synapses through complement C1q and contributed to synapse loss, dendritic spine impairment, and electrophysiology damages[23–25]. Therefore, inhibition of complement cascade may be a potential therapeutic approach to prevent sevoflurane-induced neurotoxicity.

Rutin (quercetin-3-O-rutinoside), a natural flavonoid glycoside, has different biological effects, such as antimicrobial, anticarcinogenic, antithrombotic, and neuroprotective activities[26]. It also protects individuals against memory dysfunction and depression[27,28]. Rutin can attenuate isoflurane-induced hippocampal neuroapoptosis and protect against chronic unpredictable stress-induced hippocampal neuronal loss[29,30]. Moreover, rutin can effectively relieve oxidative stress and microglia-mediated neuroinflammation in the hippocampus[28,31]. Notably, rutin exhibits excellent anticomplement properties and suppresses complement expression in transient middle cerebral artery occlusion rats[32,33]. In this study, we investigated the effects of rutin on microglial synaptic phagocytosis and sevoflurane-induced cognitive dysfunction.

Methods

Animals

The animal study was designed and conducted by relevant guidelines and regulations, including the ARVO statement for the use of animals in research and the ARRIVE guidelines. and was approved by the Institutional Animal Care and Use Committee of Nanjing University. C57BL/6J mice were sourced from Nanjing University (Nanjing, China) and were maintained in a controlled environment (12-h/12-h light/dark cycle, 21–22 °C, and 55% relative humidity) with food and water available ad libitum. Male mice were specifically chosen for the experiments. All procedures followed the Guide for the Care and Use of Laboratory Animals, outlined by Nanjing University (approved number: 2022AE01012). The sample size was determined based on another study[2].

Repeated neonatal Sevoflurane exposure and treatment

The neonatal mice were assigned randomly to either the sevoflurane group or the control group. The mice in the sevoflurane group were exposed to a mixture of 3% sevoflurane and 60% oxygen for 2 h on postnatal days 6, 8, and 10. The mice in the control group were exposed to 60% oxygen for the same duration. The concentrations of sevoflurane and oxygen were continuously supervised using a Vamos system (Dräger Medical, Germany), and the mice were kept warm at 37 ± 1 °C on a heating pad. After exposure, the mice were promptly returned to their home cages and provided regular care. For drug administration, rutin (100 mg/kg, 40 µL volume) (dissolved in phosphate-buffered saline (PBS), containing 0.1% dimethylsulfoxide (DMSO) with ultrasonication) (Yuan Ye, China) or PBS (containing 0.1% DMSO, 40 µL volume) was intraperitoneally injected into the control and sevoflurane-treated mice on PNDs 20–35 once every two days.

Cell culture and Sevoflurane exposure and treatment

Mouse BV2 microglia were obtained from Pricella Biotechnology (Wuhan, China, CL-0493). The cells were maintained in Dulbecco's modified Eagle's medium supplemented with 10% fetal bovine serum and 1% penicillin/streptomycin at 37 ℃ and 5% CO_2. For exposure to sevoflurane, BV2 cells were seeded in six-well plates and treated with 3% sevoflurane solution for 6 h as reported in another study[5]. For drug treatment, a 100 mM rutin stock solution was prepared by dissolving rutin in DMSO. Before use, this rutin stock solution was diluted in PBS to form a 1 mM working stock. After exposure to sevoflurane, the BV2 cells were washed with PBS, and the medium was renewed, which contained 100 µM rutin or complement C3 protein (100 µg/mL, HY-P7863, MCE). The cells in the control group were treated with PBS (containing 0.1% DMSO) as the vehicle control. These cells were subsequently cultured for 12 h and collected for further experiments.

CCK-8 test

BV2 cells were seeded in 96-well plates at a density of 1×10^4 cells/well and cultured with rutin for 12 h. Then, the cells were washed with PBS and cultured with a new medium containing 10 µL of CCK-8 solution (Enhanced Cell Counting Kit-8, Cat. no. C0043, Beyotime) in each well for 2 h at 37 °C. The absorbance was measured at 450 nm using a microplate reader (PerkinElmer EnSpire, Singapore), and the relative cell viability was calculated.

In vitro assay of microglial phagocytosis

BV2 cells (1×10^4 cells/well) were seeded in confocal dishes. After sevoflurane exposure and drug treatment, the cells were washed with PBS and cultured in a fresh medium containing fluorescent latex beads (1 µm, L2778, Sigma) at a concentration of 30 beads per cell mixture at 37 °C for 2 h. Subsequently, the cells were washed with PBS and fixed with 4% paraformaldehyde. Finally, images were acquired using a confocal microscope (Olympus FV1200, Japan).

Morris water maze

The MWM test was performed to evaluate the spatial learning and memorizing ability of young mice ($n = 12$) on PNDs 37–42. The operator was blinded to the group assignment. The apparatus consisted of a round steel pool (20 cm in diameter and 60 cm in height) and a platform (10 cm in diameter, 30 cm in depth). In the training phase, the mice were trained for five consecutive days with four trials each day, and the intertrial interval was 60 min. During each trial, the mice were placed in the water from various starting points, given 60 s to locate the hidden platform, and allowed to stay there for 15 s. If the mice failed to locate the platform within 60 s, they were gently guided to the platform and allowed to stay there for 15 s. In the probe test, the platform was removed, and the mice were placed in the quadrant opposite the platform and allowed to swim freely for 60 s. A video tracking system (XR-XM101, Shanghai Xinruan Information Technology Co., Ltd.) was used to record the number of entries, the proportion of time spent in the target quadrant, and the swimming speed for further analysis.

Open-field test (OFT)

The OFT was performed to assess the anxiety of the mice ($n = 12$). The open field arena was $50 \times 50 \times 40$ cm. Each mouse was placed near the wall, and its movement was recorded for 10 min using a SuperMaze Morris Video analysis system (XR-XZ301, Shanghai Xinruan Information Technology Co., Ltd). The distance traveled, average speed, and time spent in the center of the arena were calculated and analyzed.

Western blotting analysis

After conducting the behavioral tests, mice were anesthetized with 3% isoflurane, and the hippocampal tissues ($n = 5$ for each group) were collected and lysed with a lysis buffer (Beyotime, Jiangsu, China) containing protease inhibitors. The protein concentration was measured by conducting a bicinchoninic acid assay (Beyotime, Jiangsu, China). Then, 20 μg of protein was separated by SDS-PAGE and transferred onto polyvinylidene fluoride membranes. After being blocked with 5% nonfat milk (dissolved in Tris-buffered saline-Tween) for 2 h at room temperature, the membranes were washed and incubated with the following primary antibodies overnight at 4 °C: rabbit anti-PSD95 (Postsynaptic density protein-95, PSD95)(1:500; Cell Signaling Technology, 2507), rabbit anti-Vglut2 (Vesicular glutamate transporter 2, Vglut2)(1:1000; Synaptic Systems, 135402), rabbit anti-C1qa (1:1000; Invitrogen, PA5-29586), rabbit anti-C3 (1:1000; Proteintech, 21337-1-AP), rabbit anti-C4 (1:2000; Proteintech, 22233-1-AP), mouse anti-C5 (1:1500; Proteintech, 66634-1-Ig), and mouse anti-β-tubulin (1:2000; Absin, abs830032). The membranes were further incubated with horseradish peroxidase-labeled secondary antibodies: goat anti-mouse (1:1000; Beyotime, A0216) and goat anti-rabbit (1:2000; Beyotime, A0208) for 2 h at room temperature, and the protein expression was detected by Tanon 5200 (Tanon Science & Technology Co. Ltd.). The results were analyzed using the ImageJ analysis software package (version 1.8.0), and β-tubulin was used to normalize target protein expression.

Real-time quantitative PCR

Total RNAs were extracted from the hippocampus. Then, cDNA was synthesized, and real-time quantitative reverse transcription-PCR was performed as described in the previous study[2]. The primers used in this study were synthesized by Sangon Biotech and their sequences are follows: mouse C1q (forward, 5′- GGA CTG GTA TCC GAG GTT TTA A-3′; reverse, 5′- GAT ATT GCC TGG ATT GCC TTT C-3′), mouse C3 (forward, 5′- AGC TTC AGG GTC CCA GCT AC-3′; reverse, 5′- TCT CCA GCC GTA GGA CAT TG-3′), mouse C4 (forward, 5′- TGG AGG ACA AGG ACG GCT A-3′; reverse, 5′- GGC CCT AAC CCT GAG CTG A-3′), mouse C5 (forward, 5′- CAA AGG ATC CAG AAA AGA AGC CTG TAA ACC-3′; reverse, 5′ CCT TAA GCT TCG TGC AGC AGA ACT TTT CAT TC-3′) and mouse β-tubulin (5′-CAG CGA TGA GCA CGG CAT AGA C; reverse, 5′-CCA GGT TCC AAG TCC ACC AGA ATG-3′).

Immunohistochemistry

The mice were deeply anesthetized and perfused transcardially with PBS and 4% paraformaldehyde. The brains were removed to fixed with 4% paraformaldehyde for 2 h, and exposed to a cryoprotectant containing 30% (w/v) sucrose at 4 °C for 24 h. The brains were cut into 20 μm coronal sections with a Leica cryostat microtome (Leica CM1950). The sections were incubated in 5% bovine serum albumin and 0.2% Triton X solution for 2 h at room temperature. Next, the brain slices ($n = 6$ for each group) were incubated with primary antibodies at 4 °C overnight and washed with PBS. The primary antibodies used were as follows: PSD95 (1:100; 2507, Cell Signaling Technology), PSD95 (1:200, ab12093, Abcam), Vglut2 (1:200, NBP2-59330, NOVUS), C5 (1:100, Proteintech, 66634-1-Ig), and IBA1 (1:200, ab283342, Abcam). The following day, the brain sections were incubated with different secondary antibodies for 2 h at room temperature: Alexa Fluor 488-labeled goat anti-rabbit (1:200, A0423, Beyotime), Alexa Fluor 647-labeled goat anti-rabbit (1:200, A0468, Beyotime), Cy3-labeled goat anti-mouse IgG (1:200, A0521, Beyotime). Finally, the sections were stained with Hoechst 33,342 (1:1000, C1022, Beyotime) for 10 min. All images were captured under a confocal microscope (Olympus FV1200, Japan) with a 63× or 100× oil immersion objective. The percentage of the colocalization of PSD95 and Vglut2 was determined as the PSD95 and Vglut2 positive area compared to the total field area (512 pixels × 512 pixels) * 100%. The colocalization of PSD95/Vglut2 with complement was determined as the C3 and PSD95/Vglut2 positive area compared to the total field area (512 pixels × 512 pixels) * 100%.

Skeleton analysis

Confocal images of microglia were acquired using a confocal microscope (Olympus FV1200, Japan). Images were converted into single-plane maximal intensity projections and a threshold was applied. The images were subsequently processed via binarization and unsharp masking to eliminate noise. Next, they were skeletonized and the branch lengths were analyzed by the AnalyzeSkeleton plugin in ImageJ software.

Three-dimensional reconstruction of microglia and engulfment analysis

The brain sections were imaged using a confocal microscope (Olympus FV1200, Japan) with a 63× oil immersion objective. Z-stacks were acquired with a 0.5-μm step (consisting of 20–30 frames). Image stacks of the hippocampus were obtained from 3 to 4 tissues per animal ($n = 3$–4 animals per group) to reconstruct microglia (Imaris, 9.0.1, Bitplane, Switzerland). For analyzing the soma size, the IBA1 (microglia) immunoreactivity areas were outlined with a surface rendering function. A threshold was set to exclude processes precisely and a filter was used to eliminate noise. After reconstruction, the microglial soma size was determined using the analyze measure function. Double-immunostaining for microglia (IBA1) and the synaptic marker PSD95 was conducted to analyze the synaptic engulfment by microglia. Briefly, microglia and PSD95-positive synapses were reconstructed using the surface rendering function, and the PSD95 volume was co-localized within the IBA1 volume to produce a volume of synaptic engulfment in microglia. The engulfment analysis was calculated as the

volume of internalized PSD95 divided by the volume of microglia. The z-stack images were reconstructed using the Imaris software (9.0.1, Bitplane, Switzerland).

Statistics

All statistical analyses were conducted using GraphPad Prism 9 Software. All data are presented as the mean ± SEM. The Shapiro-Wilk normality test was conducted to determine whether the data followed a normal distribution. Comparisons between two groups were applied using an unpaired two-tailed t-test when data conformed to normal distribution; more than two groups' comparisons were analyzed with one-way or two-way ANOVA, followed by Tukey's post-hoc test for multiple comparisons. All differences among and between groups were considered to be statistically significant at $P < 0.05$.

Results

Rutin alleviated cognitive dysfunction in sevoflurane-treated mice

To investigate the effect of rutin (100 mg/kg) on neurocognitive deficits in sevoflurane-treated mice, an OFT was conducted on PND 37, and a Morris water maze test was conducted on PNDs 37–42 (Fig. 1A). In the OFT, mice in the control and sevoflurane groups that received PBS or rutin exhibited similar behaviors in terms of center entries, time spent in the center, and central distance traveled ($P > 0.05$, Fig. 1B, C). In the MWM test, compared to PBS injection, rutin administration decreased the time to reach the hidden platform in sevoflurane-treated mice on PNDs 38–40 (54.8 ± 6.8 vs. 42.8 ± 4.9 s, $P = 0.021$, P38; 43.1 ± 11.4 vs. 30.1 ± 10.1 s, $P = 0.004$, P39; 30.1 ± 6.1 vs. 22.4 ± 7.7 s, $P = 0.032$, P40, Fig. 1D, E). The mice treated with rutin in the sevoflurane group

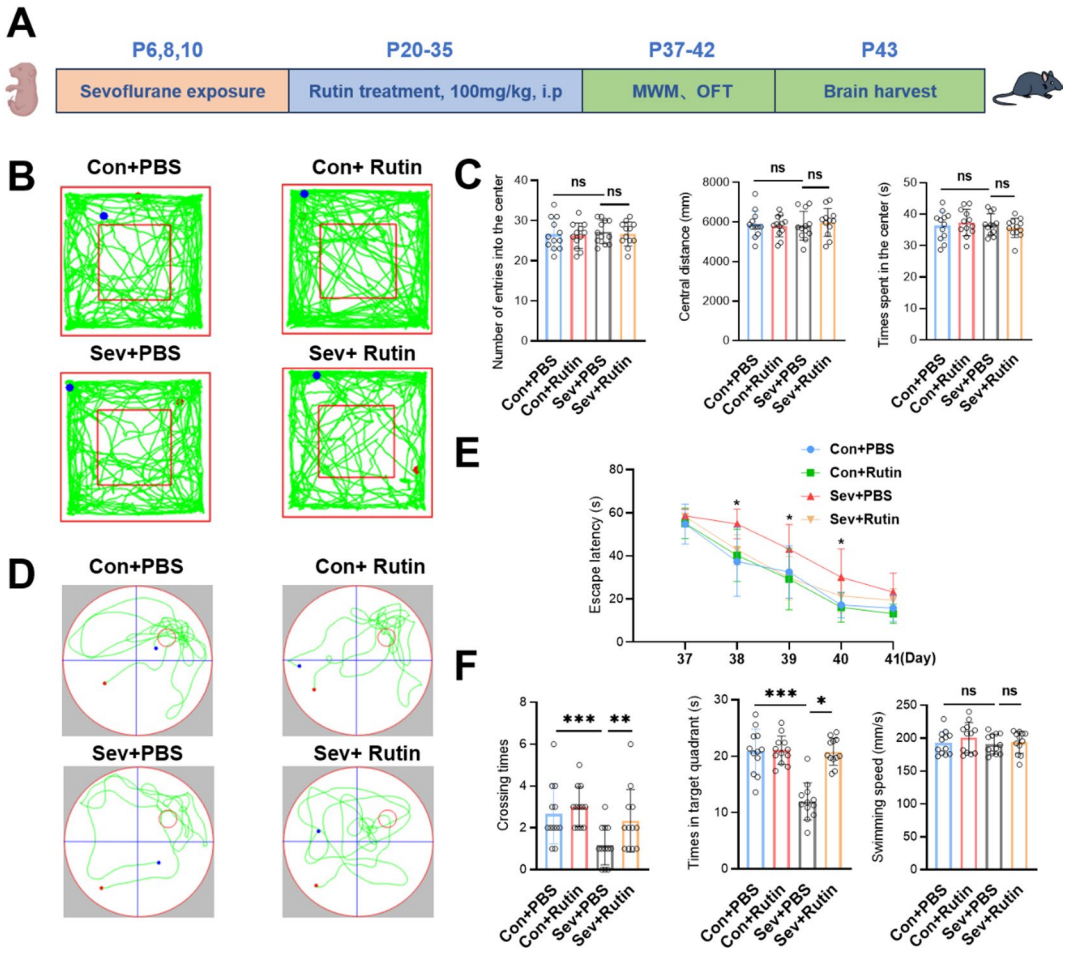

Fig. 1. Rutin alleviated cognition dysfunction in sevoflurane-treated mice. (**A**) Scheme of repeated neonatal sevoflurane exposures and the behavioral test in mice (**B**) The OF test. Representative tracking path of mice in the four groups. (**C**) Analysis of the number of entries into the center zoom, times spent in the center zoom, and central distance traveled in the four groups of mice. ($n = 12$). (**D**) MWM test. representative swimming path of mice in the four groups. (**E**) Rutin reduced the escape latency compared to treatment with sevoflurane and PBS. ($n = 12$). (**F**) Rutin increased platform cross times and time spent in the target quadrant compared to treatment with sevoflurane and PBS. ($n = 12$). One-way ANOVA or Two-way ANOVA followed by a post hoc Tukey's test was used for comparisons between the multiple groups. Data were presented as the mean ± SEM. * $P < 0.05$, ** $P < 0.01$, *** $P < 0.001$.

displayed greater platform crossing times (1.2 ± 0.9 vs. 2.3 ± 1.4 times, $P = 0.004$, Fig. 1D, F) and spent more time in the target quadrant (11.9 ± 3.2 vs. 20.7 ± 2.4 s, $P = 0.013$, Fig. 1D, F), indicating an improvement in cognitive performance. Notably, swimming speed did not differ significantly among the groups (Fig. 1F). We also compared the therapeutic effects of rutin 100 mg/kg with those of 50 mg/kg rutin. Compared to the mice in the rutin 50 mg/kg rutin group, the mice in the rutin 100 mg/kg rutin group spent less time reaching the hidden platform on PNDs 39–40 (35.37 ± 7.6 vs. 29.7 ± 8.1 s, $P = 0.034$, P39;25.32 ± 12.4 vs. 20.6 ± 7.2 s, $P = 0.083$, P40, Fig S1A, B). Additionally, the mice treated with 100 mg/kg rutin crossed the platform more times (1.6 ± 0.3 vs. 2.6 ± 0.8 times, $P = 0.037$, Fig. S1A, C) and spent more time in the target quadrant (13.8 ± 3.1 vs. 19.3 ± 2.3 s, $P = 0.003$, Fig. S1 C). These findings suggested that rutin (100 mg/kg) effectively alleviated cognitive dysfunction caused by sevoflurane.

Rutin rescued synapse loss in sevoflurane-treated mice

Recent studies have reported that prolonged and repeated sevoflurane exposure can have a detrimental effect on hippocampal development, potentially leading to behavioral deficits[34,35]. Sevoflurane exposure is linked to synaptic damage, including synapse loss, alterations in synaptic transmission, and modifications of synaptic genes. This study examined the effects of rutin on hippocampal synapses, and the result of Western blotting analysis revealed significantly greater levels of Vglut2 and PSD95 in the hippocampi of sevoflurane-treated mice than in those of PBS-treated mice ($P = 0.005$, and $P < 0.001$, Fig. 2A, B). The immunofluorescence results revealed a higher density of PSD95 and Vglut2 in the hippocampal CA1 region of sevoflurane-treated mice with rutin treatment than in control mice ($P < 0.001$, $P = 0.003$, Fig. 2C, D). Colocalization analysis of PSD95 and Vglut2 revealed that rutin significantly increased synapse density in sevoflurane-treated mice ($P = 0.004$, Fig. 2C, D). These findings suggested that rutin mitigated the hippocampal synapse impairment induced by neonatal exposure to sevoflurane.

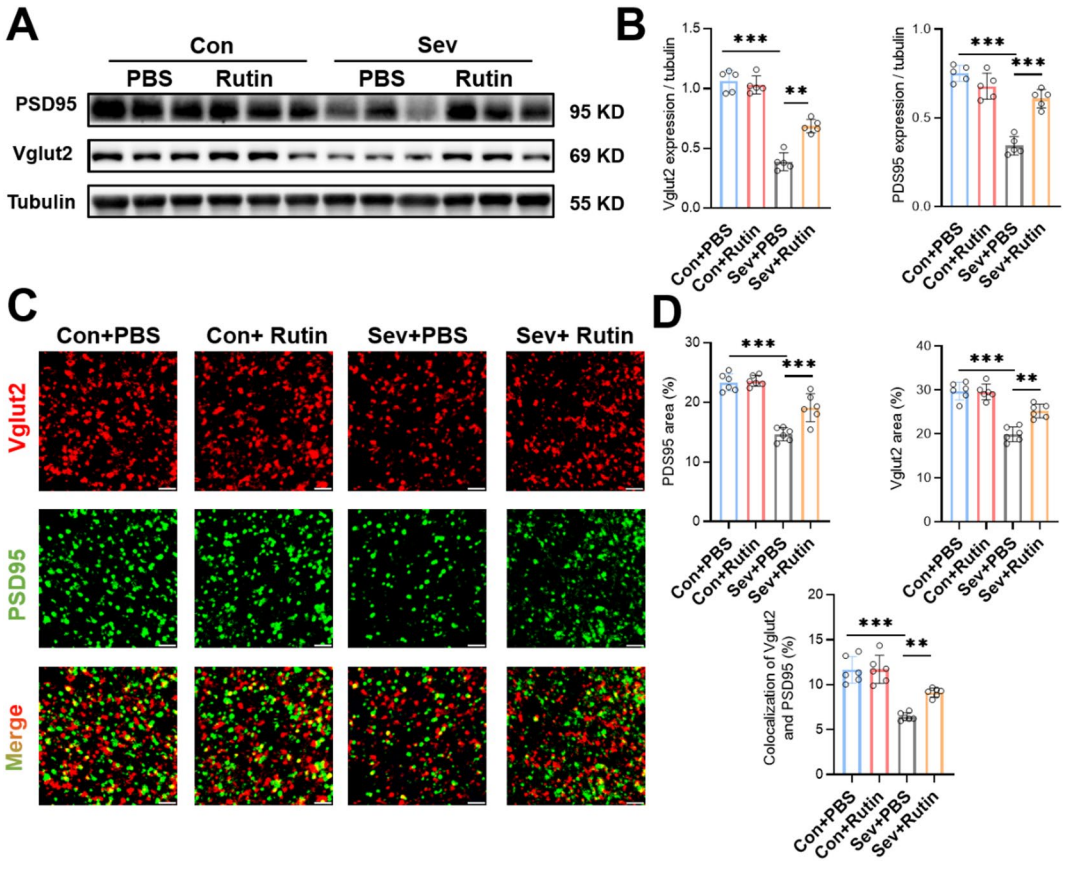

Fig. 2. Rutin rescued hippocampal synapse impairment in sevoflurane-treated mice (**A**, **B**) Western blot results showed that rutin treatment significantly increased the expression of PSD95 and Vglut2 compared to PBS in the hippocampus of sevoflurane-treated mice. ($n = 5$). (**C**) Representative confocal microscopy images of PSD95 (green) and Vglut2 (red) in the hippocampus of sevoflurane-treated mice receiving PBS or rutin. (scale bar = 5 μm). (**D**) Quantification analysis showed that compared with PBS treatment, rutin treatment increased the density of PSD95, Vglut2, and their colocalization in the hippocampus of sevoflurane-treated mice. ($n = 6$). One-way ANOVA followed by a post hoc Tukey's test was used for comparisons between the multiple groups. Data were presented as the mean ± SEM. * $P < 0.05$, ** $P < 0.01$, *** $P < 0.001$.

Rutin reduced microglial activation induced by Sevoflurane

Synapse development is strongly regulated by microglia, which help maintain the number and stability of synapses through phagocytosis[36,37]. Microglia are involved in the loss of synapses caused by sevoflurane. Sevoflurane promoted microglial engulfment by activating microglia, which resulted in the impairment of synapses. We hypothesized that rutin exerted therapeutic effects on microglia, and to test this hypothesis, we labeled microglia with IBA1 in the CA1 region and found that IBA1 intensity was significantly decreased by rutin in sevoflurane-treated mice ($P = 0.004$, Fig. 3A, B). Skeleton analysis revealed that microglia in the sevoflurane group presented an enlarged soma and shortened branches. Rutin treatment turned microglia into a highly ramified phenotype, characterized by reduced soma size and longer branches ($P = 0.03$, $P = 0.002$, Fig. 3C, D). This phenotypic switch showed that rutin reduced microglial activation caused by sevoflurane. Additionally, sevoflurane-treated

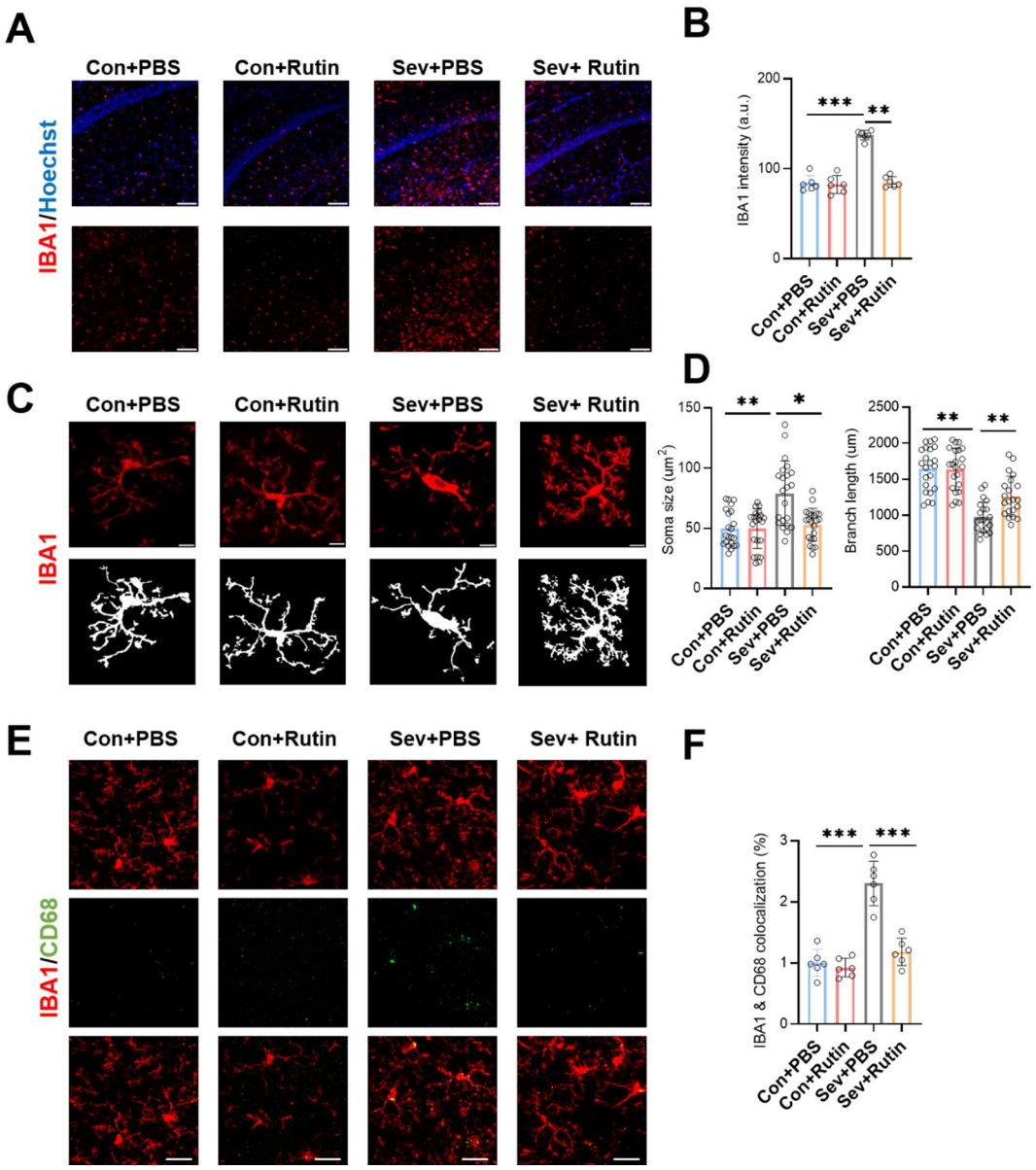

Fig. 3. Rutin reduced microglial activation induced by sevoflurane (**A**) Representative confocal images of IBA1$^+$ microglia in the CA1 region of four groups. (scale bars = 100 μm). (**B**) Quantification analysis showed that rutin led to increased IBA1 intensity in sevoflurane-treated mice. ($n = 6$). (**C**) Representative confocal images of the microglial morphology in four groups. (scale bars = 5 μm). (**D**) Quantification analysis revealed that rutin decreased microglial soma size and increased branch length, showing an inactivation phenotype. ($n = 20$). (**E**) Representative confocal images of CD68 (green) and IBA1 (red) immunoreactivity. (scale bars = 10 μm). (**F**) Quantification analysis showed that the rutin-treated mice had a lower colocalization of CD68 and IBA1 than the PBS-treated mice. ($n = 6$). One-way ANOVA followed by a post hoc Tukey's test was used for comparisons between the multiple groups. Data were presented as the mean ± SEM. * $P < 0.05$, ** $P < 0.01$, *** $P < 0.001$.

mice exhibited increased colocalization of IBA1 and CD68 (a marker of microglial activation), whereas rutin decreased their colocalization, indicating that rutin inhibited microglial activation ($P < 0.001$, Fig. 3E, F). These findings suggested that rutin effectively reduced microglial activation in sevoflurane-treated mice.

Rutin attenuated microglial phagocytosis in vitro and in vivo

Microglial synaptic engulfment is responsible for the loss of synapses in sevoflurane-treated mice. To determine whether rutin can prevent microglial synapse engulfment to rescue synapse loss, we next investigated the effects of rutin (100 μm, determined by the CCK8 test) (Fig. 4A) on the phagocytic ability of BV2 microglia. We found that BV2 cells displayed ameboid morphology (a phagocytic state) in the sevoflurane group, and rutin-treated BV2 cells exhibited highly ramified morphology (a resting state) (Fig. 4B). These changes indicated that rutin decreased the phagocytic ability of microglia. Additionally, we cocultured BV2 cells with fluorescent latex beads and found that sevoflurane increased the phagocytosis of beads by BV2 cells, whereas rutin decreased the intake of beads by BV2 cells ($P = 0.03$, Fig. 4C). To determine whether rutin prevents microglial synapse engulfment in vivo, IBA1 and PSD95 were co-stained in the CA1 region of mice. The results revealed a significant reduction (40%) in synaptic engulfment by microglia in the CA1 region of sevoflurane-treated mice receiving rutin ($P < 0.001$, Fig. 4D). These results indicated that rutin prevented microglial synaptic engulfment to reduce synapse loss in sevoflurane-treated mice.

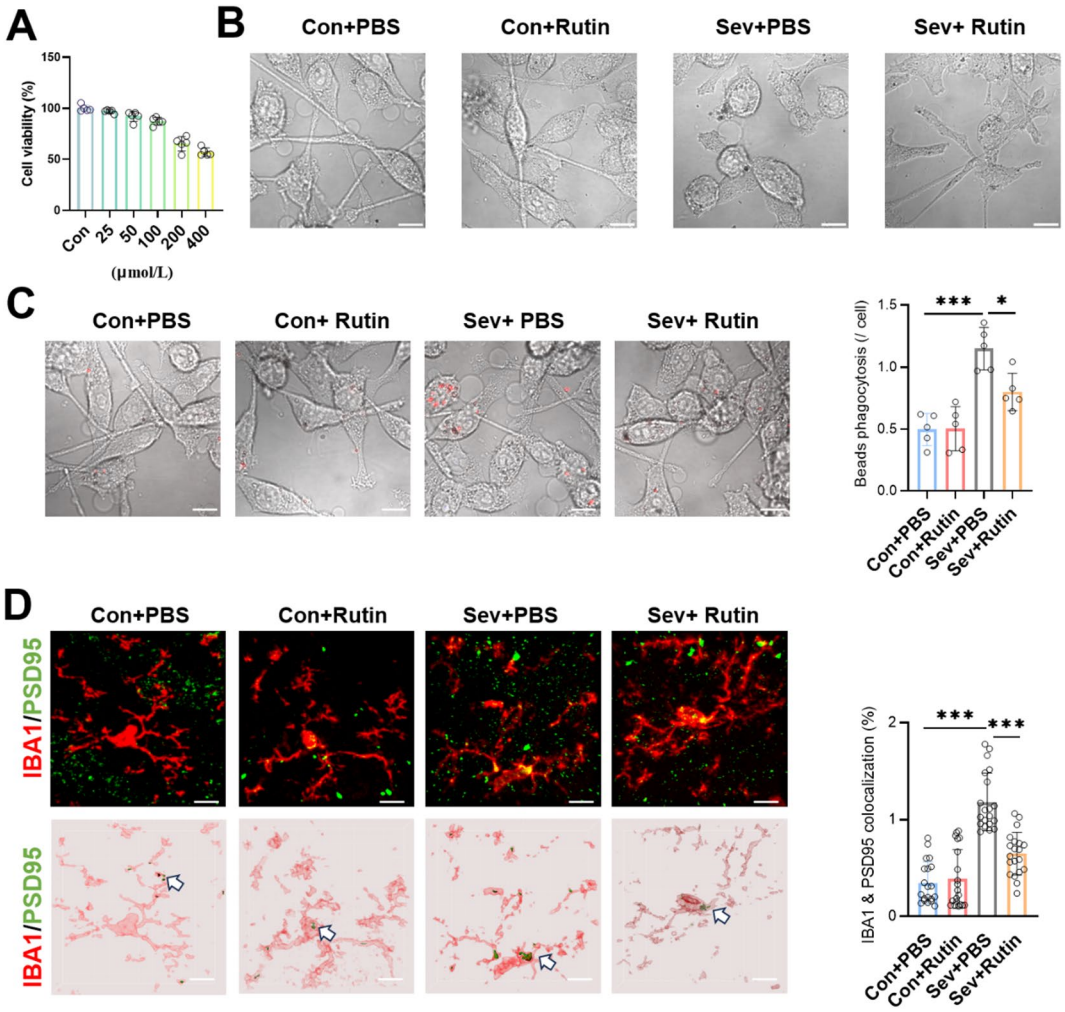

Fig. 4. Rutin attenuated the microglial phagocytosis in vitro and in vivo (**A**) The cell toxicity effect of rutin on BV2 cells. (**B**) Representative confocal microscopy images of BV2 cell morphology in the four groups. (scale bar = 15 μm). (**C**) Representative confocal images of the fluorescent latex beads phagocyted by BV2 cells in control and sevoflurane-treated BV2 cells with PBS or rutin treatment. (scale bar = 15 μm). (**D**) Representative confocal microscopy images of IBA1$^+$ (red) microglia containing PSD95$^+$ puncta (green) in the CA1 region of mice in the four groups. 3D rendering was shown. (scale bar = 5 μm). Quantification analysis showed that compared with PBS treatment, rutin treatment decreased the microglial synaptic engulfment in the sevoflurane-treated group of mice. ($n = 20$). One-way ANOVA followed by a post hoc Tukey's test was used for comparisons between the multiple groups. Data were presented as the mean ± SEM. * $P < 0.05$, ** $P < 0.01$, *** $P < 0.001$.

Rutin reduced microglial phagocytosis through the complement pathway

The classical complement cascade (C1q and C3) is involved in synapse elimination. By binding to synapses, C1q activates its downstream C3 to promote microglial phagocytosis to remove inappropriate synaptic connections[38,39]. We then detected the expression of complement C1q, C3, C4, and C5 mRNAs in BV2 cells by conducting RT-qPCR analysis. The results revealed a significant decrease in C1q and C3 mRNA levels in sevoflurane-treated mice that received rutin ($P = 0.002$, $P = 0.003$, Fig. 5A). Western blotting analysis confirmed the downregulation of C1q and C3 expression by rutin ($P < 0.001$, $P = 0.002$, Fig. 5B, C). The immunofluorescence results demonstrated that rutin decreased the C1q and C3 intensities in sevoflurane-treated BV2 cells ($P < 0.001$, $P = 0.004$, Fig. 5D, E). We subsequently added extra C3 (a downstream molecule of C1q) to the culture medium to determine whether the effects of rutin on microglial engulfment rely on complement. The results showed that extra complement C3 protein supplementation reversed the effects of rutin on microglial phagocytosis, as indicated by an increase in fluorescent bead intake by BV2 cells (Figs. 5F, S2). Moreover, sevoflurane-treated mice receiving rutin had lower C1q and C3 expression levels in the hippocampus (Fig. 6A, B). By binding to synapses, complement C3 prepares synapses for microglial engulfment. Thus, we co-labeled C3 with presynaptic Vglut2 and postsynaptic PSD95 in the CA1 region of mice. The results showed higher colocalization of C3 with PSD95 ($P = 0.002$, Fig. 6C, D) and C3 with Vglut2 ($P = 0.004$, Fig. 6E, F) in the sevoflurane group than in the control group; rutin treatment significantly reduced synaptic tagging by C3. These findings suggested that rutin suppressed the complement pathway to reduce microglial phagocytosis.

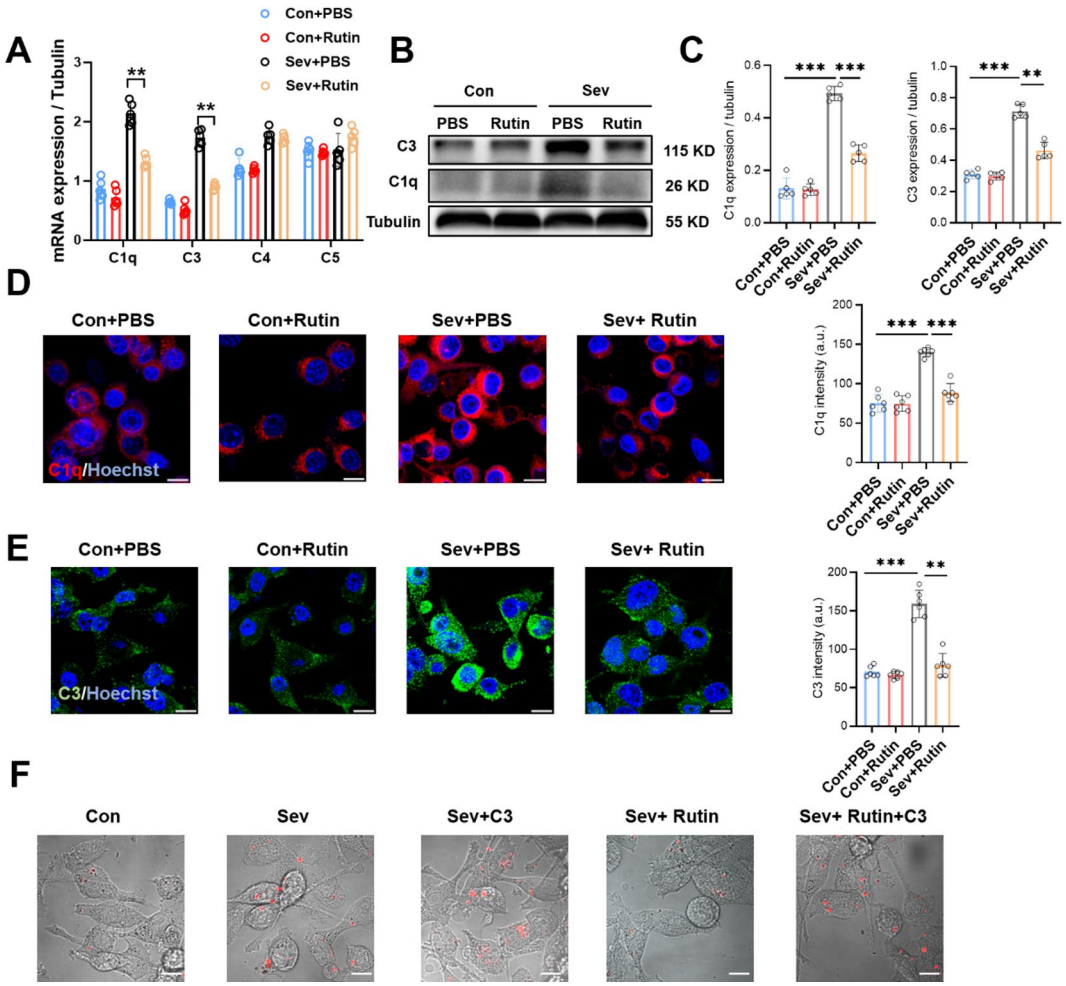

Fig. 5. Rutin suppressed the complement pathway in microglia (**A**) The mRNA expression of C1q, C3, C4, and C5 in BV2 cells in the four groups. ($n = 5$). (**B**) Representative Western blot of C1q and C3 in the four groups. (**C**) Quantification analysis showed that the expression of C1q and C3 was decreased by rutin in the sevoflurane-treated mice. ($n = 5$). (**D**) Representative confocal microscopy images and analysis of C1q in BV2 cells in the four groups. (scale bar = 15 μm). (**E**) Representative confocal microscopy images and analysis of C3 in BV2 cells in the four groups. (scale bar = 15 μm). (**F**) Representative confocal images of the fluorescent latex beads (red) phagocyted by BV2 cells in control and sevoflurane-treated BV2 cells with C3 or rutin treatment. (scale bar = 15 μm). One-way ANOVA followed by a post hoc Tukey's test was used for multiple comparisons between the groups. Data were presented as the mean ± SEM. * $P < 0.05$, ** $P < 0.01$, *** $P < 0.001$.

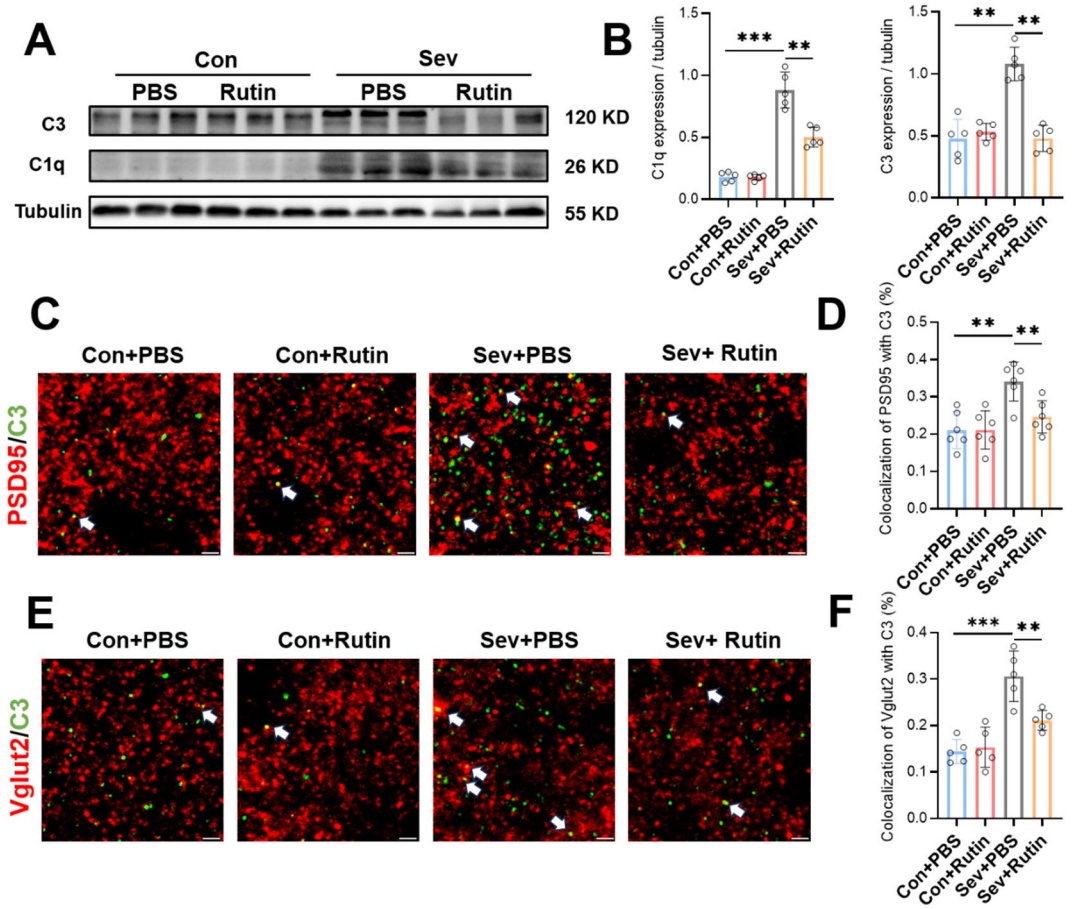

Fig. 6. Rutin reduced synapse binding of C3 (**A**, **B**) Representative Western blot and analysis of C1q and C3 in the four groups of mice. ($n = 5$). in the four groups. (**C**) Representative confocal microscopy images of PSD95 and C3 in the four groups. (scale bar = 5 μm). (**D**) Quantification analysis showed that the colocalization of PSD95 and C3 was decreased by rutin in the sevoflurane-treated mice. ($n = 6$). (**E**) Representative confocal microscopy images of Vglut2 and C3 in the four groups. (scale bar = 5 μm). (**F**) Quantification analysis showed that the colocalization of Vglut2 and C3 was decreased by rutin in the sevoflurane-treated mice. ($n = 6$). One-way ANOVA followed by a post hoc Tukey's test was used for multiple comparisons between the groups. Data were presented as the mean ± SEM. * $P < 0.05$, ** $P < 0.01$, *** $P < 0.001$.

Discussion

Exposure to anesthesia during the early postnatal period may lead to neurodevelopmental deficits, which have been widely reported[23,40,41]. Sevoflurane-induced cognitive decline is related to synaptic impairment, including synapse loss, synaptic plasticity damage, and a reduction in synaptic transmission[24,42]. In this study, our results revealed that repeated neonatal sevoflurane exposure reduced the density of synapses in the hippocampal CA1 region and negatively affected the learning and memorizing ability of young mice, which is consistent with the findings of other studies. Rutin administration also significantly alleviated synaptic impairment and cognitive dysfunction in sevoflurane-treated mice.

Several studies have revealed a role for the complement cascade in synaptic phagocytosis by microglia[43–45]. The complement proteins C1q and C3 bind to both pre-and post-synapses, and microglia then engulf C3-labeled synapses via their C3 receptors[46]. In conditions such as AD, demyelinating disease, and frontotemporal dementia, microglia eliminate synapses in a C3-dependent manner and thus contribute to pathological synapse loss[47–49]. A recent study showed that prolonged sevoflurane anesthesia upregulated C1q and C3 expression, promoted the tagging of C1q and C3 with synapses, and resulted in synapse impairment through microglial phagocytosis. Another study found that neonatal sevoflurane exposure may increase C1q expression and facilitate microglial synaptic engulfment[24,25]. Our study also showed that sevoflurane exposure increased C1q and C3 expression, and rutin treatment effectively decreased C1q and C3 levels both in vivo and in vitro. Additionally, rutin reduced the binding of C3 with pre-synaptic Vglut2 and post-synaptic PSD95.

Many experimental studies have demonstrated the importance of natural compounds in preclinical models. Rutin has been reported to exert various biological effects on neurocognitive dysfunction. In many neurological disorders, rutin has a neuroprotective effect and improves recognition memory, spatial working memory, and neurological scores[50–52]. Although the influences of rutin on neuronal or synaptic development have rarely been reported, however, rutin has been shown to exert excellent effects on microglia. Rutin pretreatment reduces

the expression of the proinflammatory cytokines and promotes the phenotypic switch of M1 microglia to M2 microglia by inhibiting the Toll-like receptor 4/nuclear factor-kappa B signaling pathway[53]. Moreover, rutin can suppress microglial activation and pyroptosis to alleviate chronic constriction injury-induced neuropathic pain[54,55]. In this study, we found that rutin effectively reduced the activation of microglia caused by sevoflurane, and promoted the shift of phagocytic microglia toward the resting phenotype. Besides its anti-inflammatory ability, rutin exhibits great anti-complement properties, with a CH_{50} value of 0.133 ± 0.021 mM[33]. Rutin can downregulate C3 levels to relieve ischemic damage and improve neurological function. Our findings indicated that rutin decreased C1q and C3 expression and reduced microglial phagocytosis i*n vivo* and in vitro, which was reversed by C3 supplementation. In AD mice, rutin has been reported to rescue synapse impairment by inhibiting microglial phagocytosis and improving pre- and post-synaptic protein levels[26]. In our study, we found that rutin reduced the binding of C3 with Vglut2 and PSD95, prevented microglial synaptic engulfment, and restored both pre-synapse and post-synapse levels. Moreover, rutin alleviated synapse loss and improved the cognition of sevoflurane-treated mice. These results indicated that rutin might be a promising candidate drug for preventing sevoflurane-induced developmental neurotoxicity.

This study had several limitations. First, we did not find changes in the number of dendritic spines caused by rutin, which is a feature of synaptic plasticity. Our further studies will investigate the effects of rutin on dendritic spine impairment. Second, we focused only on the role of rutin in microglia-mediated synaptic phagocytosis, and we can not exclude the possibility that rutin affects neurogenesis to exert its therapeutic effects. We aim to investigate this issue in the future to determine the influence of rutin on neuronal development. Finally, specific genetic interventions or inhibitors are needed to further validate the effects of rutin.

Conclusion

Our findings demonstrated that rutin inhibited complement-dependent synaptic phagocytosis by microglia to alleviate the loss of synapses and cognitive dysfunction in sevoflurane-treated mice, indicating that rutin is a promising drug candidate for treating sevoflurane-induced developmental neurotoxicity.

Data availability

The datasets used and/or analysed during the current study are available from the corresponding author on reasonable request.

Received: 25 March 2025; Accepted: 24 September 2025
Published online: 30 October 2025

References

1. Rice, D. & Barone, S. Jr. Critical periods of vulnerability for the developing nervous system: evidence from humans and animal models. *Environ. Health Perspect. 108 Suppl.* **3** (Suppl 3), 511–533. https://doi.org/10.1289/ehp.00108s3511 (2000).
2. Song, S. Y. et al. Single-nucleus atlas of Sevoflurane-induced hippocampal cell Type- and Sex-specific effects during development in mice. *Anesthesiology* **138** (5), 477–495. https://doi.org/10.1097/aln.0000000000004522 (2023).
3. DiMaggio, C., Sun, L. S., Ing, C. & Li, G. Pediatric anesthesia and neurodevelopmental impairments: a bayesian meta-analysis. *J. Neurosurg. Anesthesiol.* **24** (4), 376–381. https://doi.org/10.1097/ANA.0b013e31826a038d (2012).
4. Ing, C. et al. Long-term differences in Language and cognitive function after childhood exposure to anesthesia. *Pediatrics* **130** (3), e476. https://doi.org/10.1542/peds.2011-3822 (2012).
5. Liu, J. et al. Sevoflurane induced neurotoxicity in neonatal mice links to a GSK3β/Drp1-dependent mitochondrial fission and apoptosis. *Free Radic Biol. Med.* **181**, 72–81. https://doi.org/10.1016/j.freeradbiomed.2022.01.031 (2022).
6. Jimenez-Tellez, N. et al. Dexmedetomidine pre-treatment of neonatal rats prevents Sevoflurane-Induced deficits in learning and memory in the adult animals. *Biomedicines* **11** (2), 103390biomedicines11020391 (2023).
7. Xu, X., Li, C., Zou, J. & Liu, L. MiR-34a targets SIRT1 to reduce p53 deacetylation and promote Sevoflurane inhalation anesthesia-induced neuronal autophagy and apoptosis in neonatal mice. *Exp. Neurol.* **368**, 114482. https://doi.org/10.1016/j.expneurol.2023.114482 (2023).
8. Zhao, M. M. et al. SynCAM1 deficiency in the hippocampal parvalbumin interneurons contributes to sevoflurane-induced cognitive impairment in neonatal rats. *CNS Neurosci. Ther.* **30** (1), e14554. https://doi.org/10.1111/cns.14554 (2024).
9. Ju, X. et al. Anesthesia affects excitatory/inhibitory synapses during the critical synaptogenic period in the hippocampus of young mice: importance of sex as a biological variable. *Neurotoxicology* **70**, 146–153. https://doi.org/10.1016/j.neuro.2018.11.014 (2019).
10. Kato, R. et al. Neonatal exposure to Sevoflurane causes significant suppression of hippocampal long-term potentiation in postgrowth rats. *Anesth. Analg.* **117** (6), 1429–1435. https://doi.org/10.1213/ANE.0b013e3182a8c709 (2013).
11. Liu, Y. et al. TRPV1 antagonist prevents neonatal Sevoflurane-Induced synaptic abnormality and cognitive impairment in mice through regulating the Src/Cofilin signaling pathway. *Front. Cell. Dev. Biol.* **9** https://doi.org/10.3389/fcell.2021.684516 (2021).
12. Yu, X., Zhang, F. & Shi, J. Neonatal exposure to Sevoflurane caused cognitive deficits by dysregulating SK2 channels and GluA2-lacking AMPA receptors in juvenile rat hippocampus. *Neuropharmacology* **141**, 66–75. https://doi.org/10.1016/j.neuropharm.2018.08.014 (2018).
13. Connor, S. A. & Siddiqui, T. J. Synapse organizers as molecular codes for synaptic plasticity. *Trends Neurosci.* **46** (11), 971–985. https://doi.org/10.1016/j.tins.2023.08.001 (2023).
14. Paolicelli, R. C. et al. Synaptic pruning by microglia is necessary for normal brain development. *Science* **333** (6048), 1456–1458. https://doi.org/10.1126/science.1202529 (2011).
15. Petanjek, Z. et al. Extraordinary neoteny of synaptic spines in the human prefrontal cortex. *Proc. Natl. Acad. Sci. U S A.* **108** (32), 13281–13286. https://doi.org/10.1073/pnas.1105108108 (2011).
16. Schafer, D. P. et al. Microglia sculpt postnatal neural circuits in an activity and complement-dependent manner. *Neuron* **74** (4), 691–705. https://doi.org/10.1016/j.neuron.2012.03.026 (2012).
17. Wu, Y., Dissing-Olesen, L., MacVicar, B. A. & Stevens, B. Microglia: dynamic mediators of synapse development and plasticity. *Trends Immunol.* **36** (10), 605–613. https://doi.org/10.1016/j.it.2015.08.008 (2015).
18. Lall, D. et al. C9orf72 deficiency promotes microglial-mediated synaptic loss in aging and amyloid accumulation. *Neuron* **109** (14), 2275–2291. https://doi.org/10.1016/j.neuron.2021.05.020 (2021).
19. Wilton, D. K. et al. Microglia and complement mediate early corticostriatal synapse loss and cognitive dysfunction in huntington's disease. *Nat. Med.* **29** (11), 2866–2884. https://doi.org/10.1038/s41591-023-02566-3 (2023).

20. Zhou, J. et al. The neuronal pentraxin Nptx2 regulates complement activity and restrains microglia-mediated synapse loss in neurodegeneration. *Sci. Transl Med.* **15** (689), eadf0141. https://doi.org/10.1126/scitranslmed.adf0141 (2023).
21. Soteros, B. M. & Sia, G. M. Complement and microglia dependent synapse elimination in brain development. *WIREs Mech. Dis.* **14** (3), e1545. https://doi.org/10.1002/wsbm.1545 (2022).
22. Wen, L., Bi, D. & Shen, Y. Complement-mediated synapse loss in alzheimer's disease: mechanisms and involvement of risk factors. *Trends Neurosci.* **47** (2), 135–149. https://doi.org/10.1016/j.tins.2023.11.010 (2024).
23. Walsh, B. H. et al. Surgery requiring general anesthesia in preterm infants is associated with altered brain volumes at term equivalent age and neurodevelopmental impairment. *Pediatr. Res.* **89** (5), 1200–1207. https://doi.org/10.1038/s41390-020-1030-3 (2021).
24. Wang, G. et al. Complement C1q-mediated microglial synaptic elimination by enhancing desialylation underlies sevoflurane-induced developmental neurotoxicity. *Cell. Biosci.* **14** (1), 42. https://doi.org/10.1186/s13578-024-01223-7 (2024).
25. Xu, F. et al. Prolonged anesthesia induces neuroinflammation and complement-mediated microglial synaptic elimination involved in neurocognitive dysfunction and anxiety-like behaviors. *BMC Med.* **21** (1), 7. https://doi.org/10.1186/s12916-022-02705-6 (2023).
26. Sun, X. Y. et al. Rutin prevents Tau pathology and neuroinflammation in a mouse model of alzheimer's disease. *J. Neuroinflammation*. **18** (1), 131. https://doi.org/10.1186/s12974-021-02182-3 (2021).
27. Dimpfel, W. Rat electropharmacograms of the flavonoids Rutin and Quercetin in comparison to those of moclobemide and clinically used reference drugs suggest antidepressive and/or neuroprotective action. *Phytomedicine* **16** (4), 287–294. https://doi.org/10.1016/j.phymed.2009.02.005 (2009).
28. Koda, T., Kuroda, Y. & Imai, H. Rutin supplementation in the diet has protective effects against toxicant-induced hippocampal injury by suppression of microglial activation and pro-inflammatory cytokines: protective effect of Rutin against toxicant-induced hippocampal injury. *Cell. Mol. Neurobiol.* **29** (4), 523–531. https://doi.org/10.1007/s10571-008-9344-4 (2009).
29. Li, W. et al. Rutin attenuates isoflurane-induced neuroapoptosis via modulating JNK and p38 MAPK pathways in the hippocampi of neonatal rats. *Exp. Ther. Med.* **13** (5), 2056–2064. https://doi.org/10.3892/etm.2017.4173 (2017).
30. Parashar, A., Mehta, V. & Udayabanu, M. Rutin alleviates chronic unpredictable stress-induced behavioral alterations and hippocampal damage in mice. *Neurosci. Lett.* **656**, 65–71. https://doi.org/10.1016/j.neulet.2017.04.058 (2017).
31. Javed, H. et al. Rutin prevents cognitive impairments by ameliorating oxidative stress and neuroinflammation in rat model of sporadic dementia of alzheimer type. *Neuroscience* **210**, 340–352. https://doi.org/10.1016/j.neuroscience.2012.02.046 (2012).
32. Campanile, M. et al. Ruta graveolens water extract (RGWE) ameliorates ischemic damage and improves neurological deficits in a rat model of transient focal brain ischemia. *Biomed. Pharmacother.* **154** https://doi.org/10.1016/j.biopha.2022.113587 (2022).
33. Qin, Y. et al. Flavonol glycosides and other phenolic compounds from viola Tianshanica and their anti-complement activities. *Pharm. Biol.* **54** (7), 1140–1147. https://doi.org/10.3109/13880209.2015.1055635 (2016).
34. Jiang, Y., Zhou, Y., Tan, S., Xu, C. & Ma, J. Role of posttranslational modifications in memory and cognitive impairments caused by neonatal Sevoflurane exposure. *Front. Pharmacol.* **14**, 1113345. https://doi.org/10.3389/fphar.2023.1113345 (2023).
35. Zuo, Y. et al. Sevoflurane causes cognitive impairment by inducing iron deficiency and inhibiting the proliferation of neural precursor cells in infant mice. *CNS Neurosci. Ther.* **30** (2), e14612. https://doi.org/10.1111/cns.14612 (2024).
36. Allen, N. J. & Lyons, D. A. Glia as architects of central nervous system formation and function. *Science* **362** (6411), 181–185. https://doi.org/10.1126/science.aat0473 (2018).
37. Wilton, D. K., Dissing-Olesen, L. & Stevens, B. Neuron-Glia signaling in synapse elimination. *Annu. Rev. Neurosci.* **42**, 107–127. https://doi.org/10.1146/annurev-neuro-070918-050306 (2019).
38. Presumey, J., Bialas, A. R. & Carroll, M. C. Complement system in neural synapse elimination in development and disease. *Adv. Immunol.* **135**, 53–79. https://doi.org/10.1016/bs.ai.2017.06.004 (2017).
39. Vasek, M. J. et al. A complement-microglial axis drives synapse loss during virus-induced memory impairment. *Nature* **534** (7608), 538–543. https://doi.org/10.1038/nature18283 (2016).
40. Bong, C. L. et al. Early neurodevelopmental outcomes following exposure to general anesthesia in infancy: EGAIN, a prospective cohort study. *J. Neurosurg. Anesthesiol.* **35** (4), 394–405. https://doi.org/10.1097/ana.0000000000000857 (2023).
41. Zhou, B. et al. Astroglial dysfunctions drive aberrant synaptogenesis and social behavioral deficits in mice with neonatal exposure to lengthy general anesthesia. *PLoS Biol.* **17** (8), e3000086. https://doi.org/10.1371/journal.pbio.3000086 (2019).
42. Pappas, I., Cornelissen, L., Menon, D. K., Berde, C. B. & Stamatakis, E. A. δ-Oscillation correlates of Anesthesia-induced unconsciousness in Large-scale brain networks of human infants. *Anesthesiology* **131** (6), 1239–1253. https://doi.org/10.1097/aln.0000000000002977 (2019).
43. Borucki, D. M. et al. Complement-Mediated microglial phagocytosis and pathological changes in the development and degeneration of the visual system. *Front. Immunol.* **11**, 566892. https://doi.org/10.3389/fimmu.2020.566892 (2020).
44. Kanmogne, M. & Klein, R. S. Neuroprotective versus neuroinflammatory roles of complement: From development to disease. *Trends Neurosci.* **44** (2), 97–109. https://doi.org/10.1016/j.tins.2020.10.003 (2021).
45. Stephan, A. H., Barres, B. A. & Stevens, B. The complement system: An unexpected role in synaptic pruning during development and disease. *Annu. Rev. Neurosci.* **35**, 369–389. https://doi.org/10.1146/annurev-neuro-061010-113810 (2012).
46. Zabel, M. K. & Kirsch, W. M. From development to dysfunction: microglia and the complement cascade in CNS homeostasis. *Ageing Res. Rev.* **12** (3), 749–756. https://doi.org/10.1016/j.arr.2013.02.001 (2013).
47. Dejanovic, B. et al. Complement C1q-dependent excitatory and inhibitory synapse elimination by astrocytes and microglia in alzheimer's disease mouse models. *Nat. Aging.* **2** (9), 837–850. https://doi.org/10.1038/s43587-022-00281-1 (2022).
48. Werneburg, S. et al. Targeted complement Inhibition at synapses prevents microglial synaptic engulfment and synapse loss in demyelinating disease. *Immunity* **52** (1), 167–182 (2020).
49. Wu, Y. et al. Microglial lysosome dysfunction contributes to white matter pathology and TDP-43 proteinopathy in GRN-associated FTD. *Cell. Rep.* **36** (8), 109581. https://doi.org/10.1016/j.celrep.2021.109581 (2021).
50. Abdel-Aleem, G. A. & Khaleel, E. F. Rutin hydrate ameliorates cadmium chloride-induced spatial memory loss and neural apoptosis in rats by enhancing levels of acetylcholine, inhibiting JNK and ERK1/2 activation and activating mTOR signalling. *Arch. Physiol. Biochem.* **124** (4), 367–377. https://doi.org/10.1080/13813455.2017.1411370 (2018).
51. Ramalingayya, G. V. et al. Rutin protects against neuronal damage in vitro and ameliorates doxorubicin-induced memory deficits in vivo in Wistar rats. *Drug Des. Devel Ther.* **11**, 1011–1026. https://doi.org/10.2147/dddt.S103511 (2017).
52. Rana, A. K., Kumar, R., Shukla, D. N. & Singh, D. Lithium co-administration with Rutin improves post-stroke neurological outcomes via suppressing Gsk-3β activity in a rat model. *Free Radic. Biol. Med.* **207**, 107–119. https://doi.org/10.1016/j.freeradbiomed.2023.07.004 (2023).
53. Lang, G. P., Li, C. & Han, Y. Y. Rutin pretreatment promotes microglial M1 to M2 phenotype polarization. *Neural Regen Res.* **16** (12), 2499–2504. https://doi.org/10.4103/1673-5374.313050 (2021).
54. Ji, Y. et al. Rutin prevents pyroptosis and M1 microglia via Nrf2/Mac-1/caspase-1-mediated inflammasome axis to improve POCD. *Int. Immunopharmacol.* **127**, 111290. https://doi.org/10.1016/j.intimp.2023.111290 (2024).
55. Lim, E. Y., Lee, C. & Kim, Y. T. The antinociceptive potential of camellia Japonica leaf Extract, (-)-Epicatechin, and Rutin against chronic constriction Injury-Induced neuropathic pain in rats. *Antioxid. (Basel).* **11** (2), 103390antiox11020410 (2022).

Acknowledgements
Not applicable.

Author contributions
All authors contributed to the study conception and design. Xinyu Tian: Project administration, Formal analysis, Writing –original draft, Writing – review & editing. Miaomiao Xiong: Supervision, Writing –original draft, Writing – review & editing. Zhiguo Jiang: Supervision, Writing –original draft, Writing – review & editing. Rong Hong: Writing – review & editing. Hnghua Wang: Supervision, Conceptualization, Writing – review & editing.

Funding
Funding was supported by the Suzhou Medical Innovation and Applied Research (SKYD2022088), Suzhou Medical Association (2025YX-Q06), and Nanjing Medical University Foundation (NMUB20210269).

Declarations

Competing interests
The authors declare no competing interests.

Ethics approval
All animal experiments were approved by the Institutional Animal Care and Use Committee of Nanjing University and performed by the Guide for the Care and Use of Laboratory Animals.

Additional information
Supplementary Information The online version contains supplementary material available at https://doi.org/10.1038/s41598-025-21874-x.

Correspondence and requests for materials should be addressed to H.W.

Reprints and permissions information is available at www.nature.com/reprints.

Publisher's note Springer Nature remains neutral with regard to jurisdictional claims in published maps and institutional affiliations.